Quenching Dynamics of the Photoluminescence of $[Ru(bpy)_3]^{2+}$-Pendant PAMAM Dendrimers by Nitro Aromatics and Other Materials

Samantha Glazier, Jason A. Barron, Nelson Morales, Amy Marie Ruschak, Paul L. Houston,* and Héctor D. Abruña*

Department of Chemistry and Chemical Biology, Baker Laboratory, Cornell University, Ithaca, New York 14853-1301

Received January 10, 2002; Revised Manuscript Received December 10, 2002

ABSTRACT: The Stern−Volmer quenching constants (K_{sv}) for poly(amidoamine)- (PAMAM-) based dendrimers (generations G0−G4) modified with (4, 8, 16, 32 and 64) pendant $[Ru(bpy)_3]^{+2}$ (bpy is 2,2′-bipyridine) chromophores have been measured in the presence of three nitroaromatic quenchers (2,4,6-trinitrotoluene = TNT, 2,4-dinitrotoluene = DNT, nitrotoluene = NT), two negatively charged quenchers ($K_3Fe(CN)_6$, $Na_4Fe(CN)_6$), and one energy transfer type quencher ($Fe(C_5H_5)_2$). The quenching efficiencies were calculated for the dendrimers (G0−G4) in the presence of TNT and were found to peak for dend-16-$Ru(bpy)_3$. The generation dependence of the quenching efficiency mirrors the calculated crowding factor and the variations were attributed to changes in the 3-dimensional structure with generation (size) and the associated changes in the accessibility of the $[Ru(bpy)_3]^{2+}$-pendant groups. Electrostatic attractions between the positively charged dendrimers and the negatively charged quenchers resulted in larger K_{sv} values when compared to the reference complex, $[Ru(bpy)_3]^{2+}$. The addition of electrolyte to an ionic strength of 0.1 M (KCl or NaCl) caused a diminution of the K_{sv} values by 60%, consistent with electrostatic interactions and charge screening effects.

Introduction

TNT is a common component in low-grade explosives. Despite many advances in detection schemes, dogs still provide the most effective detection. The number of people maimed or killed by landmines provides a compelling reason to explore the development of low level, TNT-specific sensors. Detecting explosives at airports and other high-risk locations is an integral component of a larger, more comprehensive antiterrorist strategy that is under intense scrutiny at present. The work presented here is motivated by the possibility of improving future sensors using fluorescence quenching methods.

Many different classes of sensors for TNT have been developed making use of electrochemical,[1] chromatographic,[2] and spectroscopic methods.[3−5] Fluorescence quenching sensors are based on the decrease in fluorescence intensity upon the addition of an appropriate analyte quenching molecule. The high quantum yield (0.046 in water), photostability, and reducing (as well as oxidizing) power of the excited state of $[Ru(bpy)_3]^{2+}$ (bpy is 2,2′-bipyridine)

$$[Ru(bpy)_3]^{2+*} \rightarrow [Ru(bpy)_3]^{3+} + e^- \qquad E^{o\prime} = -0.85 \text{ V vs NHE}$$

$$[Ru(bpy)_3]^{2+*} + e^- \rightarrow [Ru(bpy)_3]^{+} \qquad E^{o\prime} = +0.85 \text{ V vs NHE}$$

combine to make it a very attractive fluorescence probe.

In this work we have studied five generations (0−4) of PAMAM (poly(amidoamine)) dendrimers with pendant $[Ru(bpy)_3]^{2+}$ chromophores, as well as $[Ru(bpy)]^{2+}$ in solution (as a reference material) in the presence of six different quenchers, TNT, DNT, NT, ferrocene, ferrocyanide, and ferricyanide. These were chosen for study in an effort to understand which properties, specific to dendrimers, are most desirable in sensor development and applications.

Dendrimers are highly branched molecules that form in well-defined patterns (generations) that allow control over molecular weight, topology, cavity size, and surface functionality.[6−8] There has been a great deal of effort in the synthesis and characterization of variously modified dendritic materials due to the numerous potential applications that such materials present.[9−12] Recently, the study of dendrimers has moved from the development of synthetic protocols to the application of specific functionalities.[13−17]

We are particularly interested in polypyridyl transition metal complexes, especially those of ruthenium(II), which have been extensively applied in areas such as light harvesting[18,19] and information storage[20] since they exhibit a wide range of attractive photophysical and electrochemical properties.[21−23] In this context, we have previously reported on the spectroscopic and electrochemical properties of tris(bipyridyl)ruthenium(II)-pendant PAMAM dendrimers (dend-*n*-$[Ru(bpy)_3]$) and bis(terpyridyl)ruthenium(II)-pendant PAMAM dendrimers (dend-*n*-$[Ru(tpy)_2]$ where n = 4, 8, 16, 32, and 64 for generations 0, 1, 2, 3, and 4 respectively).[24] More recently we have carried out an extensive study of the photophysics of these materials including the measurement of fluorescence lifetimes at room and low (77 K) temperatures, solvent effects and others.[25] Moreover, the ability to control molecular diameter (size), diffusion (transport), and charge without altering the nature of the chromophore by using the dendritic architecture may also point to properties to incorporate into the design of sensors. For example, since larger molecules typically diffuse at a slower rate relative to smaller molecules, one can pose the question of what would be the ideal ratio of size to mobility for minimizing the time required for collision and the subsequent quenching in diffusion-controlled quenching. The previously men-

10.1021/ma020045f CCC: $25.00
Published on Web 01/31/2003

Scheme 1. Structures and Corresponding Generation Number of Dendrimers Employed in This Study.

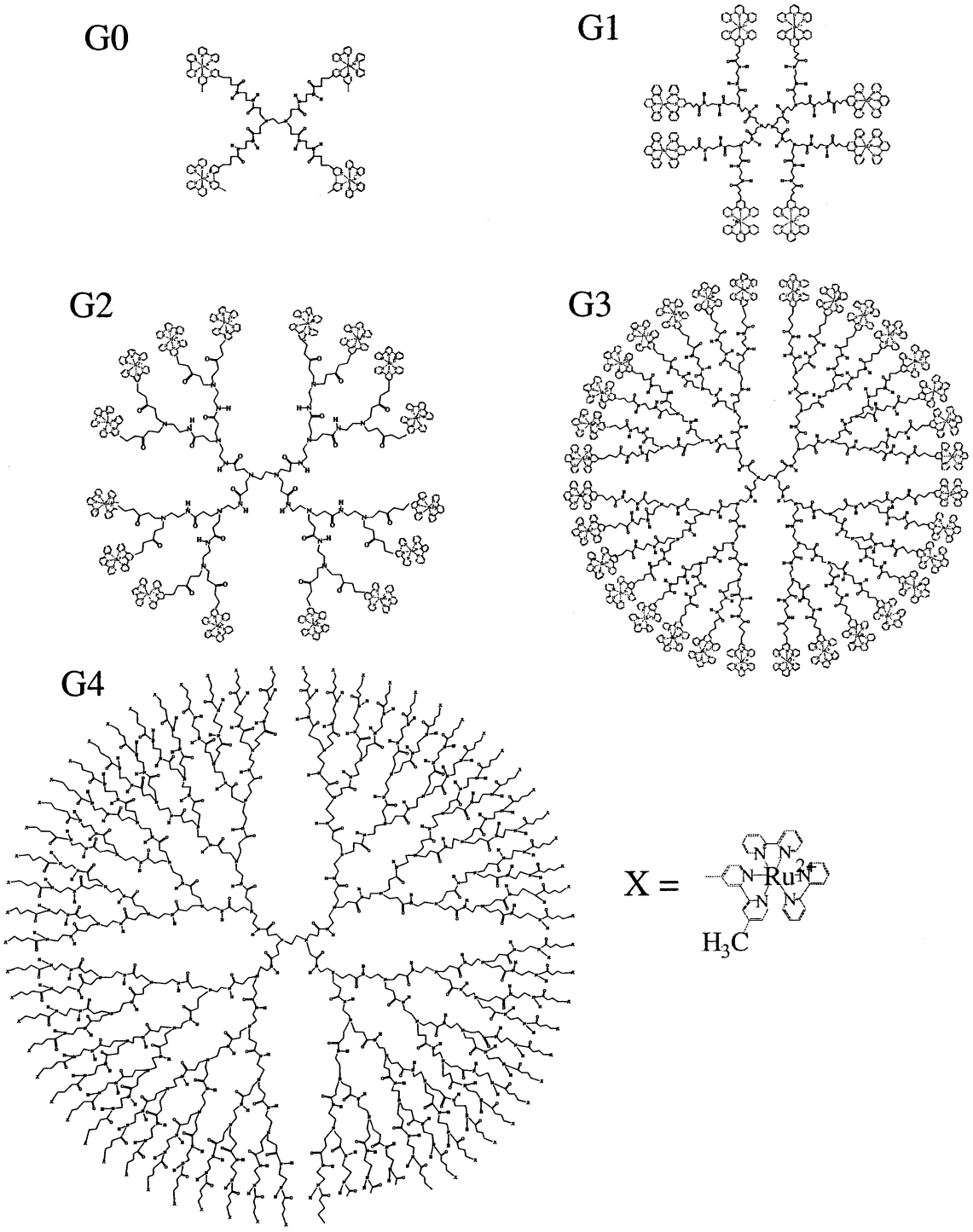

tioned studies of the photophysical properties,[25] diffusion rate constants,[26] and electrochemical analysis[24] of the [Ru(bpy)$_3$]$^{2+}$-pendant PAMAM dendrimers provide an opportunity for examining the quenching dynamics of TNT (and other quenchers) as well as insight into the behavior and reactivity of these dendritic materials, especially as a function of generation.

The focus of these investigations has been the quenching of the [Ru(bpy)$_3$]$^{2+}$-pendant dendrimer fluorescence probes by TNT and other quenchers. Of primary interest was the dependence of the quenching rate on dendrimer generation coupled with the type of quenching mechanism operative. The changes in molecular size, charge and diffusion rate constants as a function of generation is unique to a series of dendrimer generations and comprises a system capable of providing valuable insight into the most important factors controlling and affecting quenching rates.

Experimental Section

Materials. The synthesis and purification of [Ru(bpy)$_3$]$^{2+}$-pendant PAMAM dendrimers has been described previously.[24] Scheme 1 presents structures, and corresponding generation numbers, of the dendrimers employed is this study. Molecules employed as quenchers were purchased and used without further purification. Solutions of the dendrimers were prepared over a concentration range of 0.1−10 μM to maintain the same concentration of [Ru(bpy)$_3$]$^{2+}$ chromophores for all experiments. Here, 30% ethanol in water was used as the solvent for

Table 1. Quenching Data for Six Fluorophores in the Presence of Nitroaromatic Quenchers[a]

fluorophore	quencher	K_{sv} (M^{-1})[a]	k_q (M^{-1} ns^{-1})[b]	τ_o (ns)[b]	K_D (M^{-1})[b]	$10^{-10}k_o$ (M^{-1} ns^{-1})[c]
$[Ru(bpy)_3]^{2+}$	TNT	2500	3.0	800	2400	220
$[Ru(bpy)_3]^{2+}$	DNT	700				
$[Ru(bpy)_3]^{2+}$	NT	0				
dend-4-$Ru(bpy)_3$	TNT	2800	2.6	880	2250	100
dend-8-$Ru(bpy)_3$	TNT	2500	3.0	750	2300	38
dend-16-$Ru(bpy)_3$	TNT	1200	4.2	480	2000	39
dend-32-$Ru(bpy)_3$	TNT	1500	3.1	465	1500	42
dend-64-$Ru(bpy)_3$	TNT	1600	2.7	470	1250	47

[a] Superscripts refer to equation number in text.

quenching experiments with TNT (2,4,6-trinitrotoluene), DNT (2,4-dinitrotoluene), NT (nitrotoluene), and ferrocene ($Fe(C_5H_5)_2$). Millipore ultrapure water (18 MΩ) was used as the solvent when employing $K_3Fe(CN)_6$ (potassium ferricyanide) and $Na_4Fe(CN)_6$ (sodium ferrocyanide) as quenchers since they are not soluble in ethanol. The dendrimer and $[Ru(bpy)_3]^{2+}$ fluorophores were dissolved in the same solvent used for the quencher. Solutions of these were made by diluting concentrated acetonitrile solutions in either water or ethanol. All of the solutions were degassed under a flow of N_2 (99.99%) for ~20 min prior to measurement and kept under a N_2 atmosphere to prevent quenching by O_2.

The additions of quencher were made without interfering with the N_2 atmosphere by injection with a 50 μL syringe through a rubber septum attached to the sample cuvette. The concentration of the stock quencher solution was typically 5.0 mM. Small volume additions (typically 10−100 μL) were made to avoid altering the initial $[Ru(bpy)_3]^{2+}$ concentration. Five measurements, with approximately 2 min between each scan, were made for each addition.

Steady-State Emission. A SPEX 1681 Minimate-2 spectrofluorimeter with a Spectra Acq CPU controller was used for the steady-state emission measurements. The system consisted of a 150 W xenon lamp, an excitation monochromator to select the excitation wavelength (λ_{ex} = 450 nm) and an emission monochromator to scan a range of emission wavelengths (575−640 nm, λ increment of 1.0 nm, 0.5 s integration time). Slits of 1.25 and 2.50 mm width with band-passes of 4.5 and 9.0 nm were used for generations 0−2 and $[Ru(bpy)_3]^{2+}$ and for generations 3 and 4, respectively. The sample was located in a sample holder designed to minimize scattered light to the collection mirrors, positioned perpendicular to the sample that directed the fluorescence from the sample to the emission monochromator. The emission monochromator collected fluorescence in a direction perpendicular to the incident beam, and a Hamamatsu R928 photomultiplier tube operated at 1000 V was employed to detect the emission.

Time-Resolved Measurements. A Lambda Physik LPC-205i excimer laser at 308 nm and 10 Hz was used to pump a Lambda Physik dye laser using Coumarin 450 laser dye that produced 300 μJ, 20 ns fwhm pulses at 390 nm. Fluorescence was collected at 90° to the incident laser pulse by a 2 in. collection lens. Two long pass filters (OG515, OG550) were used to remove scattered laser light from the signal. A focusing lens was used to direct the fluorescence signal to a monochromator (Bausch and Lomb) set at 620 nm. The fluorescence was detected with a Hamamatsu E990-07 photomultiplier tube and the decay trace saved on a Lecroy digital oscilloscope that was triggered by a photodiode. The curves were analyzed using Origin 6.1 computer software.

Results

Fluorescence Quenching of $[Ru(bpy)_3]^{2+}$ by Nitroaromatics. Analysis of the steady-state emission data using the Stern−Volmer (SV) equation yields the SV quenching constant, K_{sv}:

$$\frac{I_o}{I} = 1 + K_{sv}[Q] \qquad (a)$$

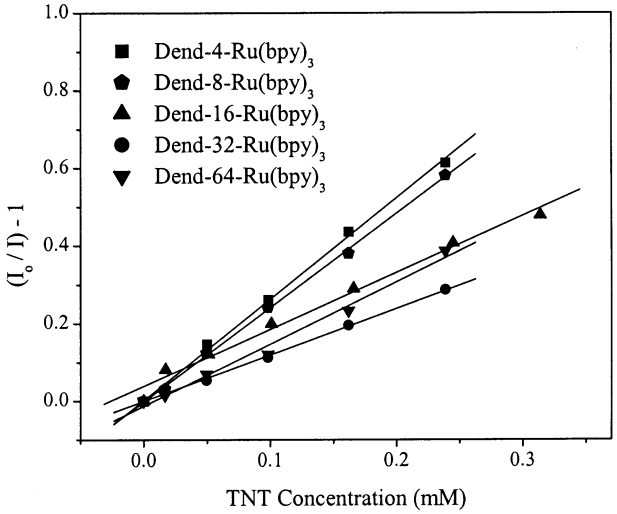

Figure 1. Stern−Volmer plots for $[Ru(bpy)_3]^{2+}$ and dend-*n*-$Ru(bpy)_3$ (*n* = 4, 8, 16, 32, 64) in the presence of TNT.

where I_0 is the emission intensity in the absence of quencher, I is the emission intensity in the presence of quencher, k_q is the bimolecular quenching constant, k_r is the radiative decay rate in the absence of any quencher, $K_{sv} = k_q/k_r$, and [Q] is the quencher concentration. Quenching data are collected and presented in Table 1. It can be seen that K_{sv} values for $[Ru(bpy)_3]^{2+}$, G0, and G1 are all near 2600 M^{-1}, while for the three largest dendrimer generations K_{sv} is near 1400 M^{-1}. Figure 1 shows SV plots of G0−G4 in the presence of TNT. The correlations were excellent with R^2 values greater than 0.99 in all cases. The solid lines in all SV plots in Figures 1, 3, and 4 represent the best fits of the data to straight lines ($R^2 > 0.99$).

To calculate the quenching rate, k_q, values of the lifetimes obtained in the presence and absence of quencher were substituted into eq b,

$$\frac{\tau_o}{\tau} = 1 + k_q\tau_o[Q] \qquad (b)$$

where τ_0 is the fluorescence lifetime in the absence of quencher and τ is the fluorescence lifetime in the presence of quencher. Figure 2 shows the linear plots obtained from eq b for G0−G4. Values of k_q and τ_o are also presented in Table 1 where it can be noted that the k_q values were approximately the same for all of the fluorescent probes. The values are centered near 3.0 M^{-1} ns^{-1} except for dend-16-$Ru(bpy)_3$ which had a measured quenching rate of 4.2 M^{-1} ns^{-1}. In agreement with previous results, τ_0 decreased with increasing dendrimer generation.[25] The dependence of the fluorescence lifetime on generation can be seen from the inset of Figure 2 that shows the decay profiles for G0−G4.

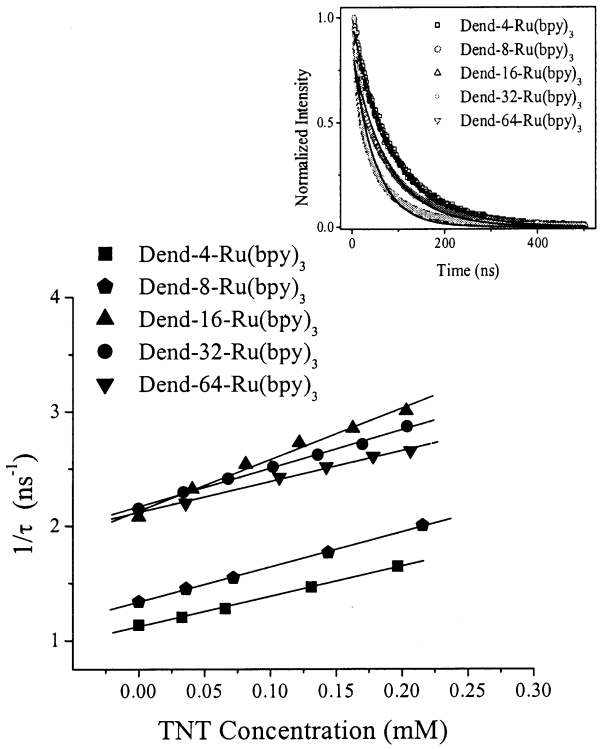

Figure 2. Plots of eq b for [Ru(bpy)$_3$]$^{2+}$ and dend-*n*-Ru(bpy)$_3$ (n = 4, 8, 16, 32, 64) in the presence of TNT. The slopes of the lines were used to determine k_q and the intercepts correspond to $1/\tau_o$. Inset: Fluorescence decay spectra at 298 K of dend-*n*-Ru(bpy)$_3$ (n = 4, 8, 16, 32, 64) in the absence of TNT. The solid lines represent the best fits of the data to single exponential decays and were used to calculate τ_o. A general decrease in the fluorescence lifetime was observed as the dendrimer generation increased.

The solid lines represents fits of the data to single exponential decays. The change in fluorescence lifetime with dendrimer generation has been attributed, at least in part, to changes in the solvation sphere around the [Ru(bpy)$_3$]$^{2+}$ chromophore. As the dendrimer generation increases, the solvent around the pendant [Ru(bpy)$_3$]$^{2+}$ groups is increasingly filled by the branches of the dendrimer with the simultaneous displacement of the bulk solvent molecules: in this case ethanol. That is, for the larger generations, the dendrimer branches function progressively more as the solvent.[27−29] The observed k_q value of 3 M^{-1} ns^{-1} is typical for diffusion-controlled quenching.[30] If the quenching were due to the formation of nonfluorescent ground state complexes (static quenching) then the lifetimes would not depend on the quencher concentration because the uncomplexed fraction would be unperturbed regardless of the number of complexes formed. Static quenching cannot account for the decrease in fluorescence intensity with increasing quencher concentration though a combination of static and dynamic quenching is possible. The lifetime measurements determined only the dynamic portion, K_D ($K_D = k_q\tau_0$), of the quenching constant and agree reasonably well, within experimental error, to K_{sv}, suggesting that static quenching does not contribute in the concentration range studied here. In addition, an upward curvature of the SV plot is observed when static quenching contributes as predicted by the quadratic equation ($I_o/I = (1 + K_D[Q])(1 + K_s[Q])$ describing combined dynamic and static quenching. All of the quenching data were adequately fit by a straight line, indicating that only dynamic quenching is significant and therefore the quenching rate depends on diffusion.

Table 2. Summary of the Crowding Factors and Quenching Efficiencies of the Fluorophores in the Presence of TNT[a]

fluorophore	f_q[d]	V_{tot} (Å^3)[e]	$V_{ca.}$ (Å^3)[f]	f_{cr}[g]
[Ru(bpy)$_3$]$^{2+}$	0.014			
dend-4-Ru(bpy)$_3$	0.026	11 680	12 250	1.39
dend-8-Ru(bpy)$_3$	0.081	23 420	26 980	0.87
dend-16-Ru(bpy)$_3$	0.108	46 920	50 360	0.93
dend-32-Ru(bpy)$_3$	0.073	93 900	84 410	1.11
dend-64-Ru(bpy)$_3$	0.056	187 900	131 100	1.43

[a] Superscripts refer to equation number in text.

Table 3. Redox Potentials of Quenching Molecules

quencher	$E^{\circ\prime}$ (V)
TNT	−0.30
DNT	−0.36
NT	−0.50
[Fe(CN)$_6$]$^{4-}$	+0.36
[Fe(CN)$_6$]$^{3-}$	+0.36
Fe(C$_5$H$_5$)$_2$	+0.37

If the molecular radii and diffusion coefficients are known, then it is a simple exercise to extract the diffusion-controlled bimolecular rate constant, k_o. This parameter may be calculated using the Smoluchowski equation,

$$k_0 = \frac{4\pi N}{1000}(R_f + R_q)(D_f + D_q) \qquad \text{(c)}$$

where R_f and R_q are the molecular radii of the fluorophore and quencher, respectively, and D_f and D_q are the respective diffusion coefficients. Using the diffusion coefficients of the fluorophores previously determined in this laboratory and estimating the radius of TNT to be about 1 nm, k_0 was calculated, and the results are shown in Table 1. The two rate constants, k_q and k_o, are related by the quenching efficiency, f_q:

$$f_q = \frac{k_q}{k_o} \qquad \text{(d)}$$

Values of the quenching efficiency are presented in Table 2 where it can be ascertained that whereas [Ru(bpy)$_3$]$^{2+}$ had the lowest value at 0.014, the value maximized at 0.18 for dend-16-Ru(bpy)$_3$.

Quenching Mechanism for [Ru(bpy)$_3$]$^{2+}$ in the Presence of Nitroaromatic Compounds. To understand the quenching mechanism of the fluorescence probes by not only TNT but also by two other nitroaromatic compounds, DNT and NT were employed as quenchers. These materials were chosen not only because of their homology with TNT but also because of the fact that they have well-defined reduction potentials that are significantly shifted from that of TNT. Table 3 shows the formal potentials for the first reduction of TNT, DNT, and NT. As can be ascertained, and as would be anticipated, TNT is the easiest to reduce, its formal potential being −0.30 V. Values for DNT and NT are −0.36 and −0.50, respectively. The Stern−Volmer analysis of the quenching data for all three nitroaromatic compounds is summarized in Table 1. The K_{sv} constant of TNT (2500 M^{-1}) is over three times larger than that for DNT (700 M^{-1}). No quenching of the [Ru(bpy)$_3$]$^{2+}$ fluorescence was observed in the case of NT. These results agree with the conclusion drawn by Whitten et al., that nitroaromatics generally behave as

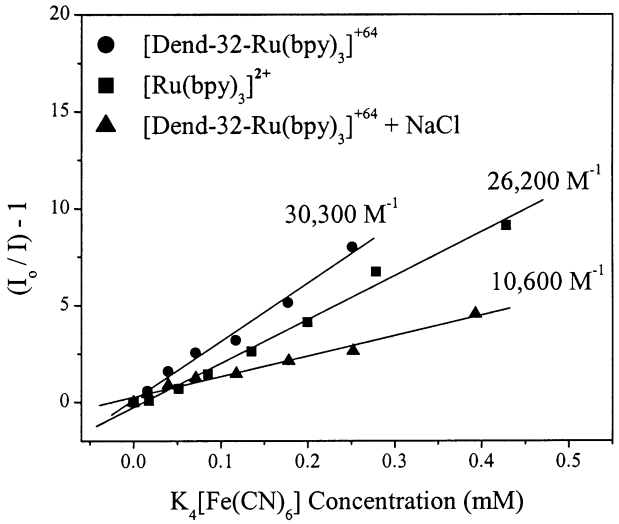

Figure 3. Stern−Volmer plots for fluorescence quenching by ferrocyanide of $[Ru(bpy)_3]^{2+}$, dend-32-Ru(bpy), and dend-32-Ru(bpy) + 0.10 M NaCl. The values of K_{sv} are shown above the corresponding lines.

Table 4. Quenching Data for Six Fluorophores in the Presence of One Neutral and Two Negatively Charged Quenchers[a]

fluorophore	quencher	K^{I}_{sv} (M^{-1})[a]
$[Ru(bpy)_3]^{2+}$	$Fe(C_5H_5)_2$	7000
dend-64-Ru(bpy)$_3$	$Fe(C_5H_5)_2$	5500
dend-64-Ru(bpy)$_3$ + 0.10 M NaCl	$Fe(C_5H_5)_2$	3600
$[Ru(bpy)_3]^{2+}$	$[Fe(CN)_6]^{4-}$	26 200
dend-32-Ru(bpy)$_3$	$[Fe(CN)_6]^{4-}$	30 300
dend-32-Ru(bpy)$_3$ + 0.10 M NaCl	$[Fe(CN)_6]^{4-}$	10 600
$[Ru(bpy)_3]^{2+}$	$[Fe(CN)_6]^{3-}$	27 400
$[Ru(bpy)_3]^{2+}$ + 0.10 M KCl	$[Fe(CN)_6]^{3-}$	10 500

[a] Superscript refers to eq in the text.

reductive quenchers.[31,32] Thus, as the formal potential of the nitroaromatic compound becomes increasingly negative, the quenching rate decreases, becoming essentially zero for the case of NT.

The quenching mechanism of $[Ru(bpy)_3]^{2+}$ by ferrocene is by energy transfer, in contrast to the either reductive/oxidative mechanisms of the nitroaromatic compounds and ferricyanide and ferrocyanide (vide infra). The K_{sv} values for quenching of $[Ru(bpy)_3]^{2+}$ (7025 M^{-1}) and G4 (6300 M^{-1}) by ferrocene (Table 4) differ only by 10%, compared to the difference of 35% between the same fluorophores in the presence of TNT. These results suggest that rate of quenching via energy transfer is somewhat less dependent on changes associated with different dendrimer generations such as molecular charge, size and diffusion rates.

Charge Effects. The molecular charge in these dendrimer generations ranges from +8 to +128. This exponential increase in charge with generation affords the opportunity to understand how to take advantage of molecular charge in designing fluorescence sensors. We approached the question in two ways. First, two negatively charged quenchers were studied to understand the effect of using oppositely and highly charged quenchers. Second, electrolyte was added in several cases to understand the effect of charge screening in the presence of neutral and negatively charged quenchers.

The negatively charged quenchers, ferrocyanide and ferricyanide, were chosen because they are known to be oxidative quenchers of $[Ru(bpy)_3]^{2+}$. The redox potentials of the compounds used as quenchers are provided

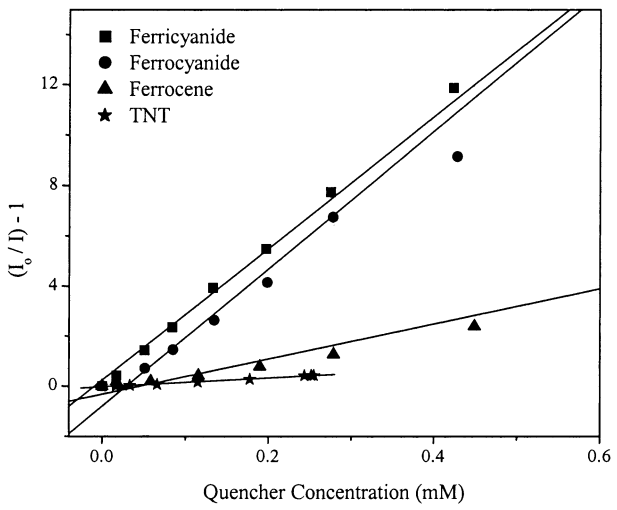

Figure 4. Stern−Volmer plots for $[Ru(bpy)_3]^{2+}$ in the presence of ferricyanide, ferrocyanide, ferrocene, and TNT.

in Table 3. The K_{sv} values obtained from steady-state measurements of $[Ru(bpy)_3]^{2+}$ in the presence of both quenchers and G3 in the presence of ferrocyanide are shown in Table 4. The SV quenching rates of $[Ru(bpy)_3]^{2+}$ are 26 200 and 27 400 M^{-1} in the presence of ferrocyanide and ferricyanide, respectively. When G3 was the fluorophore, the K_{sv} increased moderately by 15% to 30 300 M^{-1} in the presence of ferrocyanide. Figure 3 shows the slopes for the SV plots of $[Ru(bpy)_3]^{2+}$ and G3 in the presence of ferrocyanide. These results indicate that the difference in charge between the fluorophore and quencher determines, to some extent, the magnitude of the K_{sv}.

Electrolyte effects were also explored for various fluorophore/quencher combinations, and the results are shown in Table 4. In the case of the oxidative quenchers, the K_{sv} value decreased by approximately 65% when electrolyte (0.1 M) was added. Figure 3 shows the difference in slopes for the SV plots of G3 in the presence of ferrocyanide with and without added electrolyte. A less dramatic effect was observed for the neutral quencher ferrocene where the addition of electrolyte to the G4/ferrocene combination resulted in a 35% decrease in the K_{sv} value. The effects of the electrolyte in all of these systems could be rationalized as follows. First of all, it needs to be recalled that the dendrimers are highly charged species with charges that range from +8 to +128. Thus, one would, a priori, anticipate ionic strength effects due to an increased charge screening ability and concomitant diminution of the Debye length. Such effects would be even stronger for highly charged quenchers such as ferricyanide and ferrocyanide as was indeed observed. That is, there was a significant decrease in quenching (K_{sv}) upon the addition of electrolyte. The charge stabilization might provide an environment conducive to static quenching by stabilizing the nonemissive ground-state complex, which would have the same effect on the K_{sv} values. Another factor that could be at work is the diminished attraction between the quenching reactants and the subsequent decrease in collision time.

Figure 4 shows the K_{sv} plots for $[Ru(bpy)_3]^{2+}$ in the presence of ferrocyanide, ferricyanide, ferrocene, and TNT. The significant difference between the slopes of the two negatively charged quenchers and the two neutral quenchers suggest that charge is influencing the

Table 5. Quantities Used in the Theoretical Treatment of Dendrimer Branching

variable	value	description
G	0−4	generation no.
n_c	4	branching multiplicity of core moiety
n_b	2	branching multiplicity of branching moiety
V_{tot}	Table 2	total molecular vol of dendrimer
$V_{ca.}$	Table 2	conformationally available vol
v_c	4.3 Å^3	molecular vol of core moiety
v_b	18 Å^3	molecular vol of branching moiety
v_s	1450 Å^3	molecular vol of surface moiety
r_c	0.77 Å	branching radius of core moiety
l_b	5.6 Å	branch length of branching moiety
l_s	10 Å	length of surface moiety
f_{cr}	Table 2	dendrimer crowding factor

quenching rate. This is also consistent with the ionic strength effects mentioned above.

Discussion

The architecture of starburst dendrimers provokes inquiry into the dynamic conformation and changes that accompany different generations. Of note is the so-called crowding factor, f_{cr}, which is a measure of the density and steric crowding and is used to describe the change in conformation with generation.[14] Equation e gives the total molecular volume obtained by adding the volumes of the denrimer's various components. The terms are defined in Table 5.

$$V_{tot} = v_c + v_s(n_c n_b{}^g) - \frac{v_b n_c}{n_b} + \sum_{x=0}^{g} v_b n_c n_b{}^{(x-1)} \qquad \text{(e)}$$

The conformationally available space, $V_{ca.}$ (eq f), is a sphere defined by the dendrimer's core-to surface distance.

$$V_{ca.} = ({}^4/_3)\pi(r_c + g l_b + l_s)^3 \qquad \text{(f)}$$

The crowding factor is defined as $V_{ca.}/V_{tot}$ and can be reduced to eq g.

$$f_{cr} = \frac{3}{4\pi(r_c + g l_b + l_s)^3}\left[v_c + v_s n_c n_b{}^g + \frac{v_b n_c (n_b{}^g - 1)}{(n_b - 1)}\right] \qquad \text{(g)}$$

The accessibility of the [Ru(bpy)$_3$]$^{2+}$-pendant groups plays a central role in affecting f_q from eq d. Plots of f_q and f_{cr} as a function of dendrimer generation are presented in Figure 5. The peak of the quantum efficiency curve is at $f_q = 0.108$ for G2 and is reminiscent of the result that G2 is the least crowded dendrimer generation. The mirror relationship between the f_q and f_{cr} curves as a function of dendrimer generation is not surprising considering the significant role that chromophore accessibility plays in quenching efficiency. If one assumes that the more densely packed dendrimer generations have less accessible pendant groups, then the correspondence with quenching efficiency is reasonable. N. J. Turro et al. considered the effects of surface charge by measuring fluorescence quenching of donor and acceptor pairs adsorbed to the surfaces of ethylenediamine core starburst dendrimers and found a change in surface properties associated with the transformation from an open to a closed structure at approximately generation 3.[33,34] The result that the f_q is maximized at G2 could also represent a balance of molecular size, charge and diffusion rate. However accessibility appears to be the dominant factor.

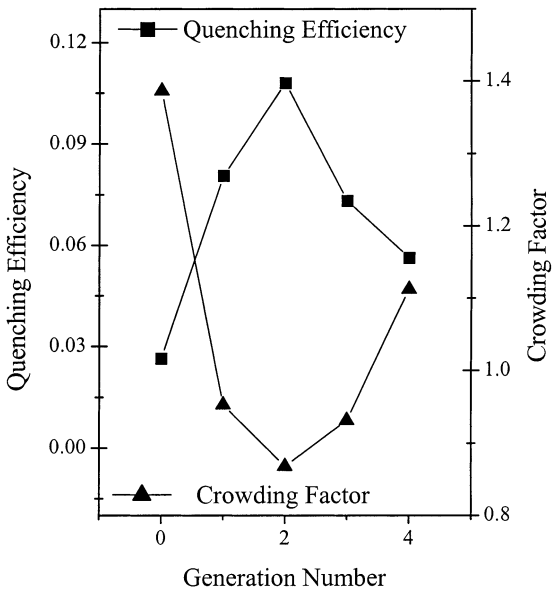

Figure 5. Quenching efficiency and crowding factor (see eqs d and g, respectively) as a function of dendrimer generation. A nearly reciprocal relationship is observed between the two quantities, indicative of the dependence of the quenching efficiency on chromophore accessibility.

Conclusions

Measurement of the quenching rates of [Ru(bpy)$_3$]$^{2+}$-pendant dendrimers in the presence of TNT, combined with the diffusion rates of the dendrimers, yielded the quenching efficiencies for generations 0−4. The most efficient quenching occurred for dend-16-[Ru(bpy)$_3$], which was also distinguished by possessing a more open structure as evidenced by the mirror relationship between the generation dependence of the quenching efficiency and the calculated crowding factor. The observed relationship was reasonable considering that the accessibility of the [Ru(bpy)$_3$]$^{2+}$-pendant groups should depend on the steric and geometric constraints accounted for by the crowding factor and that quenching efficiency depends on the accessibility of the chromophore. In addition to structural effects of the dendrimers, electrostatic attractions between the positively charged dendrimers and negatively charged quenchers resulted in larger K_{sv} values when compared to the reference complex, [Ru(bpy)$_3$]$^{2+}$. Also, the addition of 0.1 M electrolyte caused a diminution of the K_{sv} values by over 60% consistent with charge screening effects. These results show that this family of dendrimers would make excellent candidates for fluorescent probes for negatively charged quenchers.

Acknowledgment. This work was supported by the Cornell Center for Materials Research (CCMR), a Materials Research Science and Engineering Center of the National Science Foundation (DMR-9632275). N.M. and A.M.R. gratefully acknowledge the support provided by the Research Experience for Undergraduates program of the CCMR.

References and Notes

(1) Naal, Z.; Park, J.-H.; Bernhard, S.; Shapleigh, J. P.; Batt, C.; Abruña, H. D. *Anal. Chem.* **2002**, *74*, 140−148.

(2) Weisberg, C. A.; Ellickson, M. L. *Am. Lab.* **1998**, *30*, 32N-32V.
(3) Yang, J.-S.; Swager, T. M. *J. Am. Chem. Soc.* **1998**, *120*, 11864−11873.
(4) Kennedy, S.; Caddy, S. B.; Douse, J. M. F. *J. Chromatogr. A* **1996**, *844*, 97.
(5) Albert, K. J.; Walt, D. R. *Anal. Chem.* **2000**, *72*, 1947.
(6) Newkome, G. R.; Morrefield, C. N.; Vogtle, F. *Dendritic Molecules: Concepts, Syntheses, Perspectives*; VCH: Weinheim, Germany, 1996.
(7) Bosman, A. W.; Jansen, J. F. G. A.; Meijer, E. W. *Chem. Rev.* **1999**, *99*, 1665−1688.
(8) Grayson, S. M.; Fréchet, J. M. J. *Chem. Rev.* **2001**, *101*, 3819−3867.
(9) Campagna, S.; Denti, G.; Serroni, S.; Juris, A.; Venturi, M.; Ricevuto, V.; Balzani, V. *Chem.—Eur. J.* **1995**, *1*, 211−221.
(10) Cuadrado, I.; Morán, M.; Casado, C. M.; Alonso, B.; Losada, J. *Coord. Chem. Rev.* **1999**, *193*, 395−445.
(11) Vögtle, F.; Gestermann, S.; Hesse, R.; Schwierz, H.; Windisch, B. *Prog. Polym. Sci.* **2000**, *25*, 987−1041.
(12) Esfand, R.; Tomalia, D. A. *Drug Discovery Today* **2001**, *6*, 427−436.
(13) Schlupp, M.; Weil, T.; Berresheim, A. J.; Wiesler, U.-M.; Bargon, J.; Müllen, K. *Angew. Chem., Int. Ed. Engl.* **2001**, *40*, 4011−4015.
(14) Mathews, O. A.; Shipway, A. N.; Stoddart, J. F. *Prog. Polym. Sci.* **1998**, *23*, 1−56.
(15) Stoddart, F. J.; Welton, T. *Polyhedron* **1999**, *18*, 3575−3591.
(16) Smith, D. K.; Diederich, F. *Chem. Eur. J.* **1998**, *4*, 1353.
(17) Issberner, J.; Moors, R.; Vogtle, F. *Angew. Chem., Int. Ed. Engl.* **1994**, *33*, 2413.
(18) Adronov, A.; Fréchet, J. M. J. *Chem. Commun.* **2000**, *18*, 1701−1710.
(19) Gilat, S. L.; Adronov, A.; Fréchet, J. M. J. *Angew. Chem., Int. Ed. Engl.* **1999**, *38*, 1422−1427.
(20) Meyer, T. J. *Acc. Chem. Res.* **1989**, *22*, 163.
(21) Kalyanasundaram, K. In *Photochemistry of Polypridine and Porphyrin Complexes*; Academic Press: San Diego, CA, 1992.
(22) Sauvage, J.-P.; Collin, J.-P.; Chambron, J.-C.; Guillerez, S.; Coudret, C. *Chem. Rev.* **1994**, *94*, 993−1019.
(23) Balazani, V.; Juris, A.; Venturi, M.; Campagna, S.; Serroni, S. *Chem. Rev.* **1996**, *96*, 759−833.
(24) Storrier, G. D.; Takada, K.; Abruña, H. D. *Langmuir* **1999**, *15*, 872−884.
(25) Glazier, S.; Barron, J. A.; Houston, P. L.; Abruña, H. D. *J. Phys. Chem. B* **2002**, *106*, 9993−10003.
(26) Goldsmith, J. I.; Takada, K.; Abruña, H. D. *J. Phys. Chem. B.* **2002**, *106*, 8504−8513.
(27) Hecht, S.; Vladimirov, N.; Frechet, J. M. J. *J. Am. Chem. Soc.* **2001**, *123*, 18−25.
(28) Hawker, C. J.; Wooley, K. L.; Fréchet, J. M. J. *J. Am. Chem. Soc.* **1993**, *115*, 4375−6.
(29) Reitz, G. A.; Demas, J. N.; DeGraff, B. A.; Stephens, E. M. *J. Am. Chem. Soc.* **1988**, *110*, 5051−5059.
(30) Lakowicz, J. R. In *Principles of Fluorescence Spectroscopy*; 2nd ed.; Kluwer Academic/Plenum Publishers: New York, 1999.
(31) Chen, L.; McBranch, D.; Wang, R.; Whitten, D. *Chem. Phys. Lett.* **2000**, *330*, 27−33.
(32) Kim, H.-B.; Kitamura, N.; Kawanishi, Y.; Tazuke, S. *J. Phys. Chem.* **1989**, *93*, 5757−5764.
(33) Jockusch, S.; Ramirez, J.; Sanghvi, K.; Nociti, R.; Turro, N. J.; Tomalia, D. A. *Macromolecules* **1999**, *32*, 4419−4423.
(34) ben-Avraham, D.; Schulman, L. S.; Bossmann, S. H.; Turro, C.; Turro, N. J. *J. Phys. Chem. B* **1998**, *102*, 508−5093.

MA020045F